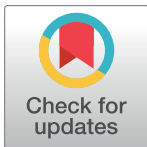# NF-kappaB Is Involved in the Regulation of EMT Genes in Breast Cancer Cells

Bruno R. B. Pires[1,2]*, **Andre L. Mencalha**[3], **Gerson M. Ferreira**[1,2], **Waldemir F. de Souza**[4], **José A. Morgado-Díaz**[4], **Amanda M. Maia**[1,2], **Stephany Corrêa**[1,2], **Eliana S. F. W. Abdelhay**[1,2]

1 Laboratório de Célula-Tronco, Instituto Nacional de Câncer José Alencar Gomes da Silva, Rio de Janeiro, RJ, Brazil, **2** Instituto Nacional de Ciência e Tecnologia para o Controle do Câncer, Rio de Janeiro, RJ, Brazil, **3** Departamento de Biofísica e Biometria, Universidade do Estado do Rio de Janeiro, Rio de Janeiro, RJ, Brazil, **4** Grupo de Biologia Estrutural, Instituto Nacional de Câncer José Alencar Gomes da Silva, Rio de Janeiro, RJ, Brazil

* brunoricardopires@gmail.com

Abstract

The metastatic process in breast cancer is related to the expression of the epithelial-to-mesenchymal transition transcription factors (EMT-TFs) SNAIL, SLUG, SIP1 and TWIST1. EMT-TFs and nuclear factor-κB (NF-κB) activation have been associated with aggressiveness and metastatic potential in carcinomas. Here, we sought to examine the role of NF-κB in the aggressive properties and regulation of EMT-TFs in human breast cancer cells. Blocking NF-κB/p65 activity by reducing its transcript and protein levels (through siRNA-strategy and dehydroxymethylepoxyquinomicin [DHMEQ] treatment) in the aggressive MDA-MB-231 and HCC-1954 cell lines resulted in decreased invasiveness and migration, a downregulation of SLUG, SIP1, TWIST1, MMP11 and N-cadherin transcripts and an upregulation of E-cadherin transcripts. No significant changes were observed in the less aggressive cell line MCF-7. Bioinformatics tools identified several NF-κB binding sites along the promoters of SNAIL, SLUG, SIP1 and TWIST1 genes. Through chromatin immunoprecipitation and luciferase reporter assays, the NF-κB/p65 binding on TWIST1, SLUG and SIP1 promoter regions was confirmed. Thus, we suggest that NF-κB directly regulates the transcription of EMT-TF genes in breast cancer. Our findings may contribute to a greater understanding of the metastatic process of this neoplasia and highlight NF-κB as a potential target for breast cancer treatment.

Introduction

Breast cancer is the leading cause of cancer death among women worldwide. According to GLOBOCAN, this neoplasia is responsible for 522,000 deaths in women each year [1]. Late diagnosis increases the risk of cancer cells spreading from the primary tumor to neighboring tissues and distant organs in a process known as metastasis. In breast cancer, almost all deaths are attributed to metastasis, which is responsible for 90% of deaths from solid tumors [2]. Metastasis involves sequential and interrelated steps: cancer cells develop an invasive growth,

detach from the primary tumor, degrade the basement membrane, migrate into the circulatory system (intravasation), evade immune attack, and escape from capillaries (extravasation) to invade and proliferate in distant organs [3].

The epithelial-to-mesenchymal transition (EMT) is considered one of the major mechanisms involved in solid tumor metastasis. During the EMT, tumor cells lose their epithelial features and acquire a mesenchymal phenotype leading to invasive and migratory behavior. The earliest events of the EMT include the downregulation of cell-cell adhesion molecules, such as the adherens junction protein E-cadherin, and upregulation of weak adhesion related molecules, such as N-cadherin and vimentin. In addition, matrix metalloproteinases (MMPs), which are capable of degrading the extracellular matrix (ECM), are upregulated. This phenotype switch is a reversible process regulated mostly by the transcription factors *SNAIL1*, *SLUG (SNAIL2)*, *TWIST1* and *SIP1 (ZEB2)*, which downregulate epithelial markers and upregulate mesenchymal markers and MMPs [4–9]. Moreover, overexpression of these transcriptional factors in breast cancer has been correlated with higher histologic grade, lymph node metastasis and poor survival [10–12].

The intense cell migration and invasion during metastasis have characteristics common with those of cell movements during embryogenesis. During *Drosophila* sp. development, dorsal acts as a transcriptional activator of *snail* and *twist*, which are crucial to gastrulation [13,14]. The mammalian ortholog of *dorsal* is the nuclear factor-κB (NF-κB) family. However, the regulatory mechanisms of this modulation have not yet been demonstrated in human cancers.

The NF-κB family has been described as a critical regulator of a large number of biological processes, including cell proliferation, differentiation, immune responses and inflammation. This family consists of five subunits: p50 (NF-κB1), p52 (NF-κB2), p65 (RelA), c-Rel (Rel) and RelB, which associate to form functional homo- and heterodimers. The NF-κB complex is usually inactive and located in the cytoplasm while bound to IκB inhibitor proteins. For the NF-κB complex to be released from its inhibitor, the IκB protein must be phosphorylated by the IκB kinase (IKK) complex, which leads to IκB ubiquitination and subsequent degradation by the 26S proteasome. NF-κB is then translocated into the nucleus and activates gene transcription by binding to sequence-specific target DNA [15] known as κB sites (5′-GGGRNYYYCC-3′, where R: purine, Y: pyrimidine and N: any nucleotide) [16]. This complex has more than 150 regulatory target genes, and the most abundant heterodimer found is the p65/p50 complex [17,18]. Recently, a positive correlation between EMT transcription factors and NF-κB activation has been described in several human cancers [19]: breast cancer [20], prostate cancer [21], renal carcinoma [22], and head and neck squamous cell carcinomas [23]. However, there is no evidence to date on how NF-κB regulates EMT-inducing factors.

Pharmacological and genetic approaches are commonly applied to study specific cell signaling. The NF-κB inhibitor DHMEQ (dehydroxymethylepoxyquinomicin), which is a derivative of the antibiotic epoxyquinomicin C [24], directly binds to NF-κB/p65 and specifically represses its nuclear translocation and its DNA-binding activity [25,26]. DHMEQ has a unique specificity in blocking NF-κB activity [15], and preclinical studies on cancer cell lines or in xenograft settings have shown effective growth inhibition in several tumors, such as breast cancer [27], prostate cancer [28], bladder cancer [29], thyroid cancer [30], pancreatic cancer [31], head and neck carcinoma [32], multiple myeloma [33] and adult T-cell leukemia [34]. Due to its chemical properties and biological activity, the use of DHMEQ has been promising for *in vitro* studies and clinical procedures. In this study, the specific properties of DHMEQ as an NF-κB/p65 inhibitor were utilized to specifically affect this transcriptional factor. Moreover, interference technology, such as siRNA, can also produce direct effects on one target and allow the evaluation of its downstream-regulated genes and phenotype.

Here, we sought to examine the impact of NF-κB inhibition on the tumoral properties of human breast cancer cells and to determine how NF-κB regulates the expression of EMT transcription factors. The inhibition of NF-κB (using DHMEQ and siRNA strategies) decreased EMT-TF levels in the aggressive cells. Moreover, a significant binding of NF-κB to the *SLUG*, *TWIST1* and *SIP1* promoter regions was observed, and the activation of these genes by NF-κB through promoter activity was confirmed using a luciferase reporter strategy. Altogether, our results provide evidence regarding NF-κB's transcriptional involvement in EMT-TF regulation.

Materials and Methods

Cell lines and culture

The human breast cancer cell lines MCF-7 (ATCC HTB-22), HCC-1954 (ATCC CRL-2338) and MDA-MB-231 (ATCC HTB-26) were cultured in RPMI-1640 (Sigma-Aldrich) supplemented with 10% fetal bovine serum (FBS), 2 mM glutamine, 100 units/ml penicillin and 100 μg/ml streptomycin. The cells were cultured in a humidified 5% CO_2 atmosphere at 37˚C.

Chemicals

DHMEQ, the NF-κB/p65 inhibitor, was synthesized as previously described [16]. All the cell lines studied were subjected to treatment with DHMEQ and evaluated in various conditions described in the manuscript.

Cell viability assay

Different concentrations (3, 10 and 30 μg/ml) of DHMEQ were used to investigate the dose-response effect. We determined the cell viability with the colorimetric WST1 (water-soluble tetrazolium salt) kit according to the manufacturer's instructions (Roche).

Cell migration assay

To address the contribution of NF-κB/p65 to cancer cell migration, a wound healing assay was performed. Briefly, breast cancer cells were seeded into a 6-well plate and cultured as described above. Cell monolayers at 90% confluence were wounded by scratching them with a 200 μl plastic tip, washed with phosphate buffered saline (PBS), and incubated in fresh culture medium supplemented with 1% FBS to prevent proliferation [35] in the presence or absence of DHMEQ (10 μg/ml). Cell cultures were photographed (x100 magnification) 24 h after wounding using an Axio Observe.Z1 microscope equipped with an AxioCam HRc and the AxioVision Release 4.8 digital image processing software (Carl Zeiss Inc.). The relative width of the wounds was obtained as the average distance between edges, and the original wound width (0 h) was defined as 100% [35]. The experiments were performed in triplicate.

Cell invasion assay

A Matrigel transwell invasion assay was performed to examine the effect of NF-κB/p65 inhibition on the cell invasion process. Approximately 10^4 cells were seeded in medium containing 1% FBS in the presence or absence of DHMEQ (10 μg/ml) onto the upper region of the transwell chamber (8-μm pore size; Corning) coated with a Matrigel basement membrane-like matrix (1 mg/ml; BD). The lower chamber of the transwell was filled with medium containing 10% FBS. After a 24-h incubation at 37˚C and 5% CO_2, the cells were fixed with absolute ethanol and stained with crystal violet, and the non-invaded cells present in the inserts were removed with a cotton swab. Images of the invaded cells were acquired using the same equipment described above. Five random fields

were photographed (x200 magnification) and counted. The values of non-treated cells were defined as 100%, and the relative proportion was calculated for DHMEQ-treated cells. The experiments were performed in triplicate.

Real-time reverse transcription polymerase chain reaction (RT-qPCR) analysis

The mRNA levels of cells were investigated by RT-qPCR. Briefly, total RNA was purified using the TRIzol reagent (Invitrogen) according to the manufacturer's instructions. Then, 2 μg of RNA was processed using the DNase Amplification Grade I Kit (Invitrogen) to remove DNA contamination and was reverse transcribed into cDNA using the Superscript-III First Strand Synthesis kit (Invitrogen) following the manufacturer's protocol. RT-qPCR was performed with the SYBR Green Master Mix (Invitrogen) in a Rotor-Gene Q (Qiagen), and the conditions were as follows: 95˚C for 10 min, followed by 40 cycles of 30 s at 95˚C, 30 s at 60˚C and 30 s at 72˚C. Each sample was examined in triplicate. The primers used are described in S1 Table. *ACTB* and *GAPDH* were used as the reference genes for the mRNA levels. Fold-expression was calculated according to the $\Delta\Delta C_t$ method [36].

Prediction of NF-κB binding regions

To screen for putative NF-κB binding sites along 1,000 bp upstream of the transcription start site of *SNAIL1*, *SLUG*, *SIP1* and *TWIST1* genes, we used on-line prediction tools. The on-line software used included the following: Transfac (http://www.gene-regulation.com), Tfsitescan (http://www.ifti.org/cgi-bin/ifti/Tfsitescan.pl), TESS (http://www.cbil.upenn.edu/cgi-bin/tess/tess), TFBind (http://tfbind.hgc.jp/) and TFSearch (http://www.cbrc.jp/research/db/TFSEARCH.html). The DNA sequences of the promoter regions were acquired from the NCBI database (www.ncbi.nlm.nih.gov). The alignment among species was performed using the Ensembl orthology tool (www.ensembl.org).

Chromatin immunoprecipitation (ChIP)

To confirm the predicted NF-κB binding sites, ChIP assays were conducted as described previously [37]. Briefly, the lysed and digested material was incubated with 5 μg of NF-κB/p65 antibody (C-20, sc-372, Santa Cruz Biotechnology) or with a negative immunoprecipitation control normal rabbit IgG (#2729, Cell Signaling). We next purified the DNA using microcolumns and subjected it to qPCR, employing specific primers for each putative NF-κB binding site listed in S2 Table. Reactions were performed under the same conditions as described above. The fold-change of the NF-κB-precipitated sample was calculated in relation to the IgG-precipitated control. Both samples were normalized by the input C_t [38]. Each sample was examined in triplicate.

Luciferase reporter assay

The plasmids used for this experiment were as follows: pGL3-Promoter Vector, pGL3-plasmid containing *SLUG*, *SIP1* or *TWIST1* promoter regions (cloned as described below) and an internal control pRL-TK renilla luciferase expression plasmid (Promega). Each DNA promoter region was amplified by PCR from human genomic DNA with the primers listed in S2 Table. For promoter constructs without predicted sites, we used the following primers: *SLUG* promoter -398 bp forward 5'-GGCTCTCATTAACACCAGAGG-3' and +5 bp reverse 5'-CCTTTACGAACTGAGCCCG-3'; *TWIST1* promoter -38 bp forward 5'-TCCTCCTCACGTCAGGC-3' and +29 bp reverse 5'-GTCTGGGAGTTGGGCGAGA-3'; and SIP1 promoter -636 bp forward 5'-TCCCTGCTAAGTTTCTCTATGGC-3' and +22 bp reverse 5'-CCTTGAAGTCTCCGCAAACG-3'. The

PCR products were inserted into the PCR 2.1 TOPO plasmid (Invitrogen). Next, they were digested with XhoI and SacI (Promega) and inserted into the corresponding sites of pGL3-Promoter Vector using T4 DNA ligase (Invitrogen). We co-transfected 0.2 μg of pGL3-Promoter Vector or pGL3-DNA promoter with 0.2 μg of pRL-TK Renilla plasmid in MDA-MB-231 cells with Lipofectamine LTX with Plus Reagent (Invitrogen). The extracts were prepared from cells 48 h after transfection of the constructs using a Dual-Luciferase Reporter Assay System (Promega) to measure luciferase enzyme activity in a Veritas Microplate Luminometer (Turner Bio-Systems) according to the manufacturer's instructions. Luciferase activity was expressed as relative light units, the firefly luciferase was normalized to the renilla vector, and the values were reported relative to the pGL3 (Mock) signal. All of the experiments were performed in triplicate.

NF-κB/p65 knockdown

To knockdown NF-κB/p65 *in vitro*, specific short interference RNA (siRNA) was used (sc-29410, Santa Cruz Biotechnology). A siRNA that does not match any known human coding cDNA was used as a negative control for silencing (Scramble, sc-37007, Santa Cruz Biotechnology). Transfections were performed using Lipofectamine LTX (Invitrogen) as per the manufacturer's instructions, 4×10^5 cells were plated in a 6-well plate containing RPMI-1640 media without antibiotics, and transfections were conducted with 50 nM of NF-κB/p65 siRNA (or Scramble) for up to 72 h.

Immunoblotting

Whole-cell protein extracts were obtained from cell lines in lysis buffer containing 50 mM Tris pH 7.5, 5 mM EDTA, 10 mM EGTA, 50 mM NaF, 20 mM b-glycerolphosphate, 250 mM NaCl, 0.1% Triton X-100, 20 mM Na_3VO_4 and protease inhibitor mix (Promega). The protein concentrations were determined using the Bradford assay, and 30 μg of the cell lysate proteins was separated by 12% sodium dodecyl sulfate-polyacrylamide gel electrophoresis (SDS-PAGE). The proteins were transferred to nitrocellulose membranes (Bio-Rad), blocked with 5% milk and incubated with the anti-NF-κB/p65 (ab16502-100, Abcam) and anti-Slug (C19G7, Cell Signaling) antibodies at 1:1000 dilutions. Antibody binding was detected using ECL reagents (Thermo Scientific). Images were acquired using Image Studio Digits software v 3.1 with a LI-COR instrument (Uniscience). Rouge Ponceau staining was used to assess equal loading.

Statistical analysis

All of the data were expressed as the mean ± standard deviation (SD) of at least three independent experiments and analyzed by a two-tailed Student's t-test using GraphPad Prism v.5 (GraphPad Inc., USA). *p*-values <0.05 were considered statistically significant.

Results

NF-κB/p65 inhibition decreases the malignant potential of breast cancer cells

DHMEQ was used to inhibit NF-κB/p65 activity through its binding and repression of nuclear translocation and its DNA-binding activity. Initially, we evaluated the dose-response of DHMEQ in the cell lines used in this study through a cell viability assay (WST1 kit, Roche) and an NF-κB/p65-luciferase reporter assay (we performed a luciferase reporter assay, as described in the Materials and Methods section, using a construct containing NF-κB response elements fused to the luciferase gene [39]) (S1 and S2 Figs, respectively). DHMEQ at 10 μg/ml inhibited NF-κB activity

without significantly affecting the cell viability. Therefore, this concentration was used in all of the experiments.

To evaluate the role of NF-κB/p65 in the regulation of the malignant potential of breast cancer cells, the cells were treated with DHMEQ (10 µg/ml), and wound healing migration and Matrigel transwell invasion assays were subsequently conducted. As seen in Fig 1, treatment with DHMEQ decreased the motility of MDA-MB-231 (Fig 1A) and HCC-1954 (Fig 1B) cells (1.36- and 1.88-fold, respectively). Furthermore, an important reduction of their invasive potential (3.26- and 2.86-fold, respectively) was observed (Fig 2A and 2B). Nevertheless, the migratory and invasive potential of MCF-7 cells was not significantly affected after treatment with DHMEQ (Figs 1C and 2C). Together, these data suggest that NF-kB/p65 can influence the aggressive features in breast cancer cells.

NF-κB/p65 inhibition reduces SLUG, TWIST1 and SIP1 expression and reverts the EMT expression pattern

As our experiments indicated that NF-κB/p65 is important for the cell migratory and invasive properties of breast cancer cells (Figs 1 and 2), we questioned whether NF-κB/p65 inhibition would alter EMT-related gene expression. For this purpose, we conducted pharmacological inhibition of NF-κB through DHMEQ treatment in MDA-MB-231, HCC-1954 and MCF-7 cells. We found that *SLUG*, *TWIST1* and *SIP1* transcript expression was decreased at 8 h of DHMEQ treatment in MDA-MB-231 cells (Fig 3A) and HCC-1954 (Fig 3B). Our findings also showed an upregulation of the epithelial marker *E-CAD* and downregulation of *N-CAD* and *MMP11* for both cell lines (Fig 4A and 4B). To further strengthen our data and evaluate a direct role of NF-κB, we performed NF-κB knockdown in the same cell models. As shown in Fig 5, the gene expression profile obtained for *SLUG*, *TWIST* and *SIP1* after pharmacological inhibition of NF-κB was also observed after its silencing through siRNA, further suggesting that NF-κB supports the EMT expression pattern. *SNAIL1* expression was not significantly altered for any condition in any cell line. Moreover, no significant changes were observed in the less aggressive cell line MCF-7 (S3A, S3B and S3C Fig).

NF-κB protein expression was evaluated in both strategies applied to silence its signaling. As shown in Fig 3 and Fig 5, a reduction in NF-κB/p65 expression was observed for both cell lines, suggesting a downregulation in the signaling pathway. Additionally, the downstream target SLUG was also evaluated, and its expression was reduced in siNF-κB MDA-MD-231 cells (Fig 5A).

In silico determination and ChIP confirmation of NF-κB binding sites in the SLUG, TWIST1 and SIP1 promoter regions

To predict κB sites in the promoter regions of the previously investigated EMT-inducing factors, we used several bioinformatics tools. We identified four NF-κB binding consensus sequences in the *SNAIL* promoter (-124, -430, -834 and -1119 bp) (Fig 6A), two in the *SLUG* promoter (-587 and -783 bp) (Fig 6B), six in the *TWIST1* promoter (-54, -249, -870, -956, -983 and -997 bp) (Fig 6C) and three in the *SIP1* promoter (-769, -1111 and -1339 bp) (Fig 6D). Alignment analyses revealed that the proximal regions were highly conserved among metazoan species.

To address whether NF-κB binds directly to the predicted sites in the *SNAIL1*, *SLUG*, *TWIST1* and *SIP1* promoters, we performed a ChIP assay followed by qPCR (ChIP-qPCR) using the MDA-MB-231 (Fig 7A), HCC-1954 (Fig 7B) and MCF-7 (S3C Fig) cell lines. Consistent with the mRNA levels of EMT-inducing factors, a significant binding of NF-κB to *SLUG* -587 bp, *TWIST1*–54 bp and *SIP1*–769 bp sites was observed in both the MDA-MB-231 and
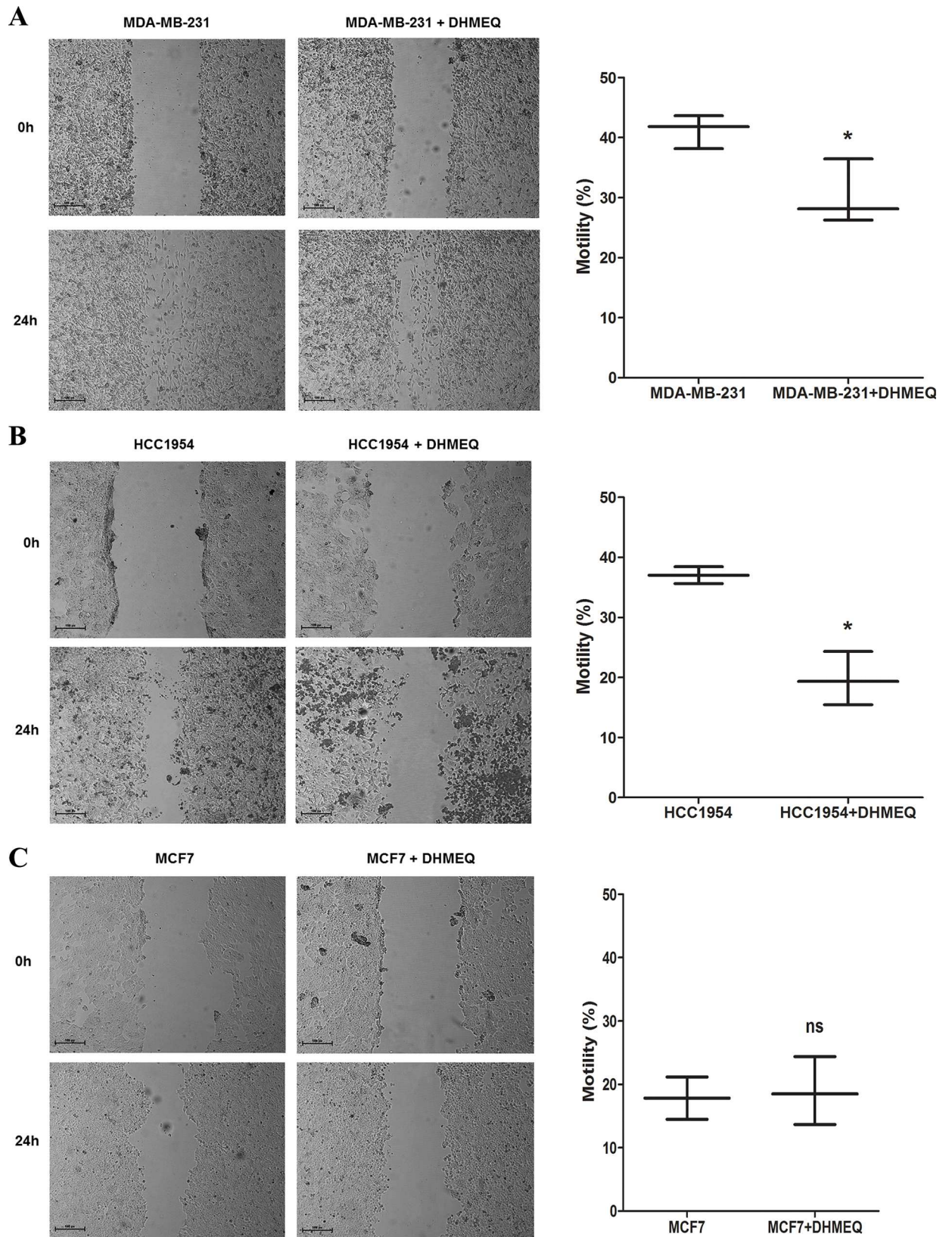
Fig 1. Migration assay. A representative wound healing assay evaluating cell migration at 24 h after DHMEQ treatment of MDA-MB-231 (A) HCC-1954 (B) and MCF-7 (C) cells is shown. The box plots represent migratory ability as indicated by the percent of wound closure. Magnification x100. The data were expressed as the mean ± SD. * = $p<0.05$, ns = not statistically significant.

doi:10.1371/journal.pone.0169622.g001

HCC-1954 cell lines. No predicted site in the *SNAIL1* promoter region was shown to be an NF-κB binding site, and the same result was found for the *SLUG* -783, *TWIST1*–249 and *SIP1*–1111 bp sites in all of the studied cell lines. Then, the NF-κB inhibitor was used to confirm the specificity of NF-κB binding to the selected sites. DHMEQ treatment decreased the enrichment of all of the sites tested in the ChIP samples, resulting in signals similar to the basal levels found in the IgG negative control (Fig 7). ChIP assays performed in MCF-7 cells did not show significant binding of NF-κB to any of the predicted sites (S3C Fig). These observations confirmed the *TWIST1* promoter -54 bp, *SLUG* promoter -587 bp and *SIP1* promoter -769 bp sites as direct transcriptional targets of NF-κB in aggressive breast cancer cells.

Activation of the SLUG, TWIST1 and SIP1 promoters by NF-κB

We examined *SLUG*, *TWIST1* and *SIP1* promoter activity using a luciferase reporter plasmid containing a proximal promoter fragment upstream of the luciferase gene. These constructs were transfected transiently into MDA-MB-231 cells with or without DHMEQ. As shown in Fig 8, we observed an increase in the promoter activity of SLUG -587, TWIST1–54 and SIP -769 when addressing NF-κB binding sites, suggesting the participation of NF-κB as a regulator of these EMT-TFs' expression. These results were confirmed by a decrease in luciferase activity in DHMEQ-treated cells. These results corroborate the sites defined by ChIP as NF-κB binding sites.

Discussion

The EMT is described as critical for the early stages of metastasis by regulating the cellular morphology and the gain of invasive/migratory potential by cancer cells [40–42]. Another property of cells undergoing the EMT is the secretion of proteases, such as MMPs, which cleave the protein components of the ECM, favoring migration. Concomitantly, the upregulation of mesenchymal markers, such as N-cadherin, and downregulation of E-cadherin provide a spindle shape to tumor cells, which facilitates their interaction with the ECM during the invasion of adjacent tissues [40,41]. It is noteworthy that after reaching their secondary site, cells undergo the mesenchymal-to-epithelial transition (MET) and acquire an epithelial phenotype similar to that of the primary tumor [40]. This process is characterized by a high phenotypic plasticity, which can be triggered by signals from the microenvironment [40–42].

The role of EMT-TFs has been consistently demonstrated in both xenograft models and human tumors [41]. In breast cancer, the role of these factors has been described during progression and metastasis. In addition, increased levels of SNAIL, SLUG, TWIST1 and SIP1 expression are related to poor prognosis and a higher risk of recurrence [10–12, 41].

We characterized NF-κB/p65 as a transcriptional regulator of the main EMT-inducing factors related to metastatic progression in breast cancer: SLUG, SIP1 and TWIST1. These results were corroborated by inhibition of NF-κB/p65 with DHMEQ, which reduced the migration and invasiveness of the aggressive breast cancer cells MDA-MB-231 and HCC-1954. Inhibition of NF-κB/p65 also changed the pattern of expression of EMT markers in both cell lines, resulting in reduced levels of SLUG, SIP1, TWIST1, N-cadherin and MMP11 concomitant with augmented levels of the epithelial marker E-cadherin. Indeed, NF-κB inhibition usually results in a reduction of the aggressive features of breast cancer, as demonstrated by others [43–45]. Our findings also support the potential of NF-κB inhibition for breast cancer treatment, which was intensively studied by Umezawa's group through both *in vitro* [46] and *in vivo* [27] experiments.
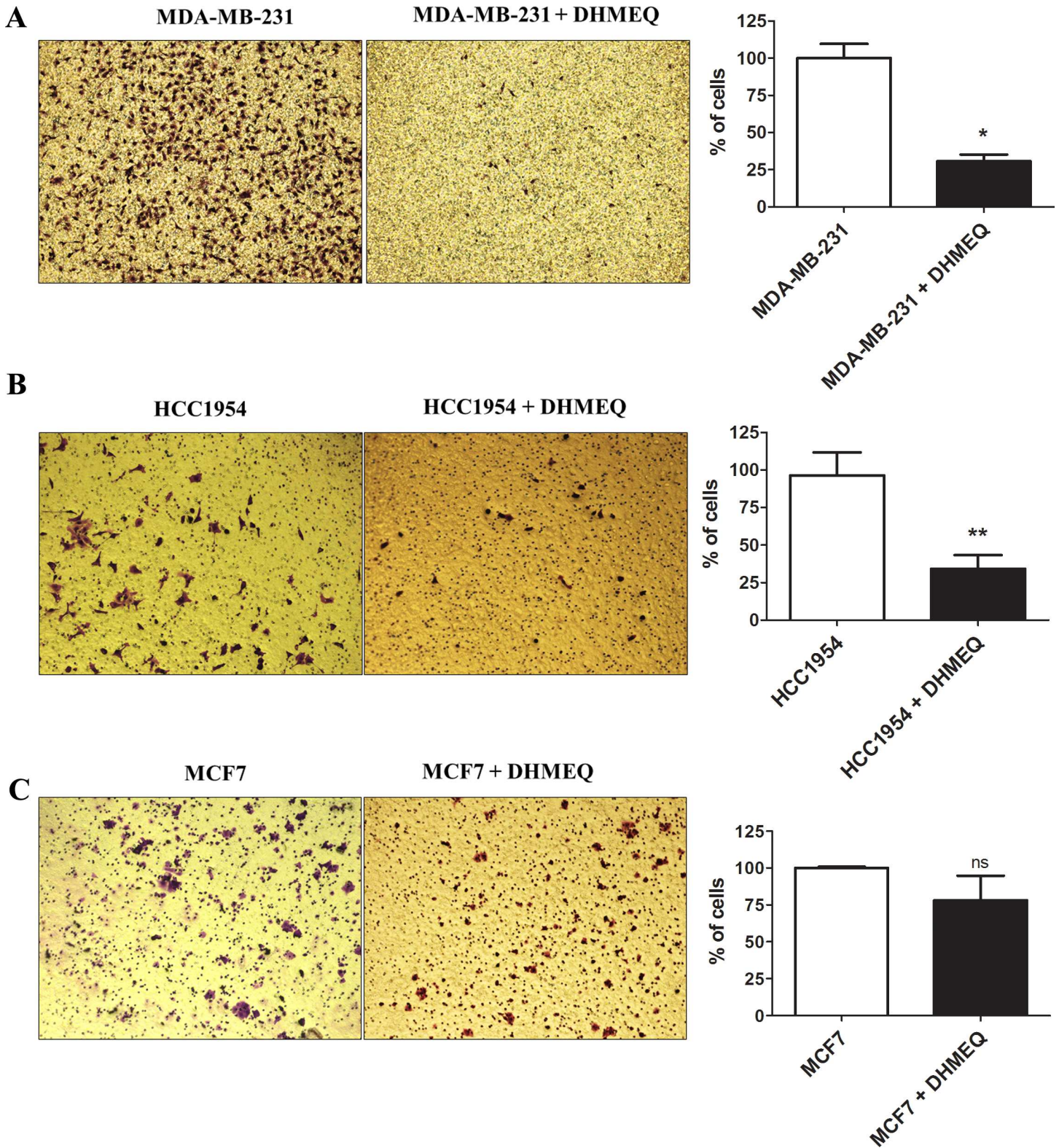
Fig 2. Invasiveness assay. A representative Matrigel transwell assay evaluating invasive potential at 24 h after DHMEQ treatment of MDA-MB-231 (A) HCC-1954 (B) and MCF-7 (C) cells is shown. The bar graph represents the relative invasive potential of MDA-MB-231, HCC-1954 and MCF-7 cells. The cells were stained with crystal violet. Magnification x200. The data were expressed as the mean ± SD. * = $p<0.05$, ** = $p<0.01$, ns = not statistically significant.

doi:10.1371/journal.pone.0169622.g002
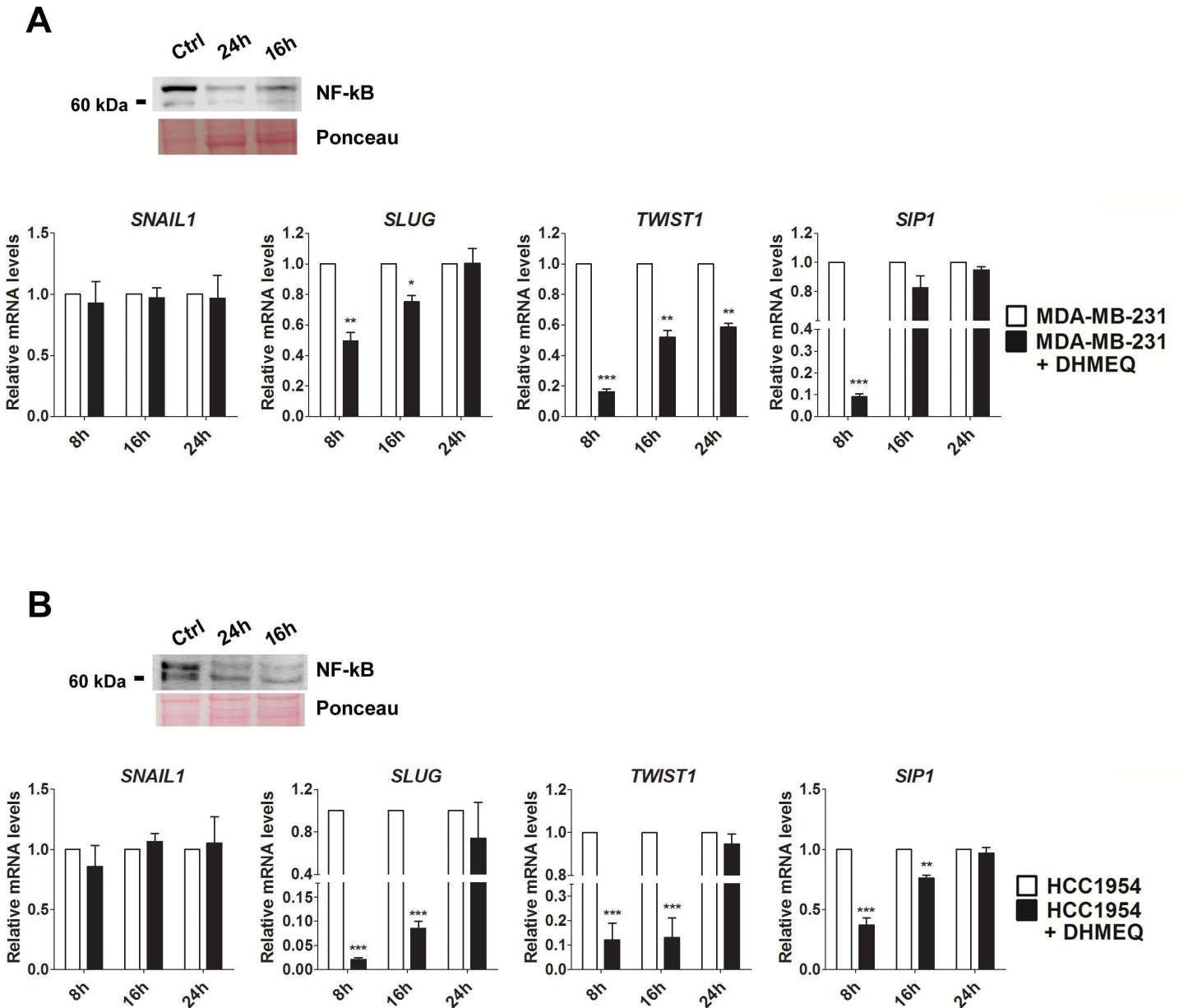
Fig 3. Relative expression of the EMT-inducing factors after NF-κB/p65 signaling inhibition. The mRNA levels of *SNAIL1*, *SLUG*, *TWIST1*, and *SIP1* were assessed in MDA-MB-231 (A) and HCC-1954 (B) cells at 8, 16 and 24 h of DHMEQ treatment. NF-κB/p65 inhibition was evaluated at protein levels by western blot assay at 16 and 24 h of DHMEQ treatment. Ponceau staining was used as a loading control. Ctrl: control. The data were expressed as the mean ± SD. * = *p*<0.05, ** = *p*<0.01, *** = *p*<0.001.

doi:10.1371/journal.pone.0169622.g003

Consistent with previous studies using human cancer models [47–49], our results showed that NF-κB inhibition was unable to change the expression of Snail in human breast carcinoma cells (Fig 3), although a correlation between these transcription factors has been demonstrated during the embryonic development of *Drosophila* sp. [13], *Xenopus laevis* [50] and *Danio rerio* (zebrafish) [51].

NF-κB inhibition not only decreased the motility and invasiveness of MDA-MB-231 and HCC-1954 cells (Figs 1 and 2) but also reduced the expression of EMT markers in a significant manner (Figs 3 and 4). In contrast to the results obtained for the aggressive cell lines, MCF-7
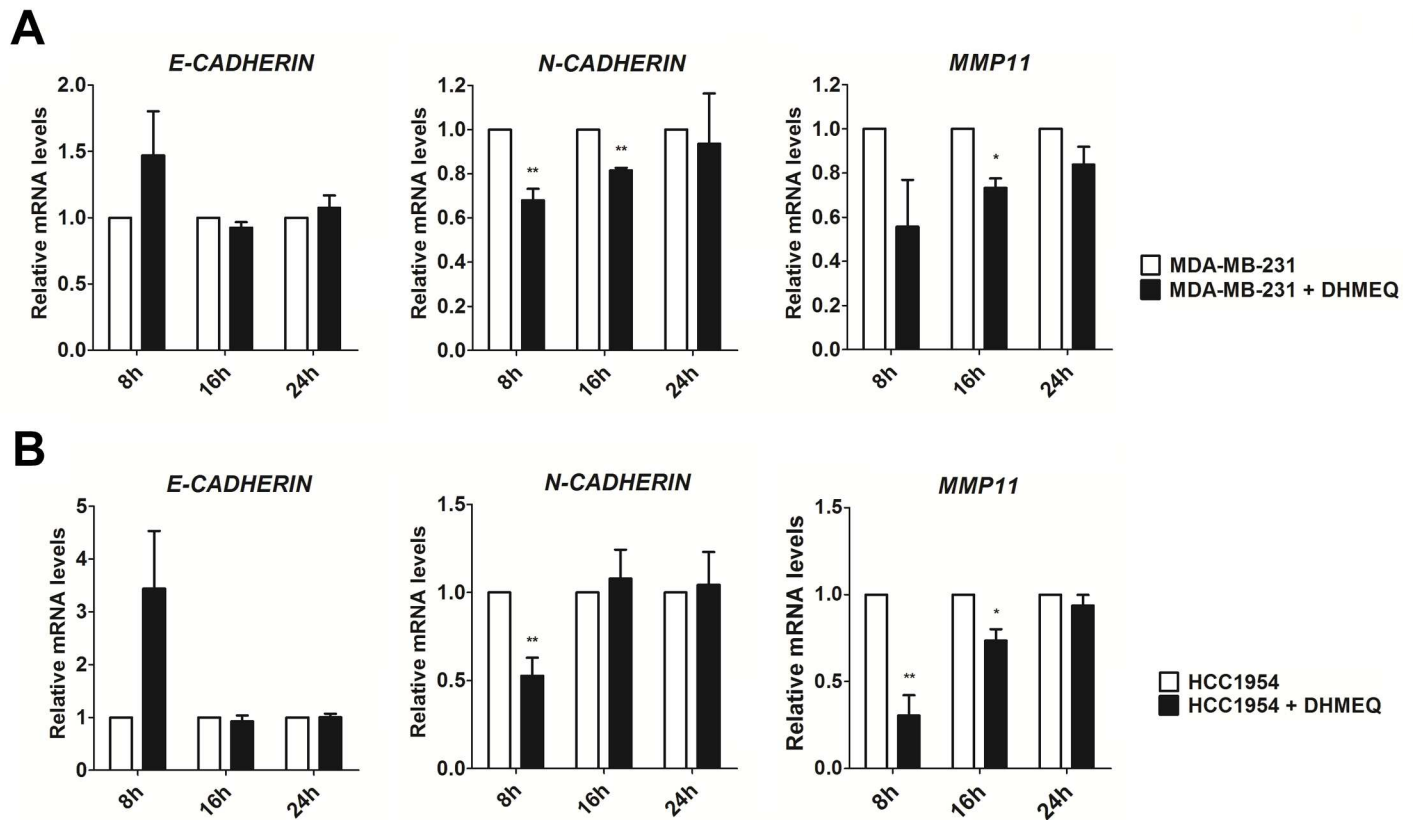
Fig 4. Relative expression of EMT-phenotype markers after NF-κB/p65 signaling inhibition. The mRNA levels of *E-CADHERIN*, *N-CADHERIN* and *MMP11* were assessed in MDA-MB-231 (A) and HCC-1954 (B) cells at 8, 16 and 24 h of DHMEQ treatment. The data were expressed as the mean ± SD. * = *p*<0.05, ** = *p*<0.01, *** = *p*<0.001.

doi:10.1371/journal.pone.0169622.g004

cells (which are less aggressive than the other cell lines) treated with DHMEQ showed no change in the migratory and invasiveness cellular assays or in the expression of EMT-associated genes (Figs 1 and 2 and S3 Fig). This finding can be explained by the fact that MCF-7 is described as expressing low levels of endogenous NF-κB [27] and EMT-inducing factors [7,52–54], which was confirmed by our group using RT-qPCR (data not shown).

The possible direct regulation of EMT-TFs by NF-κB has been discussed, although it has not been demonstrated experimentally to date. Huber et al. [43] demonstrated a strong correlation between NF-κB and EMT using a murine model of mammary carcinoma transfected with the oncogene c-Ras. These findings allowed the same authors [55, 56] to hypothesize that NF-κB might regulate EMT factors.

Computational predictions are an important tool to identify putative binding sites. Because different algorithms developed by different bioinformatics tools have been used, a great volume of data has been generated, which may show different or identical results. To solve this conflict, we focused on the more frequent and consensus sites among these bioinformatics tools. The predicted NF-κB binding sites were evolutionarily conserved among metazoan species, indicating a biological relevance of these regions throughout evolution (Fig 6). Furthermore, the data obtained by ChIP-qPCR assays (Fig 7) and confirmed by the luciferase promoter activity assays (Fig 8) showed strong evidence that NF-κB/p65 transcriptionally
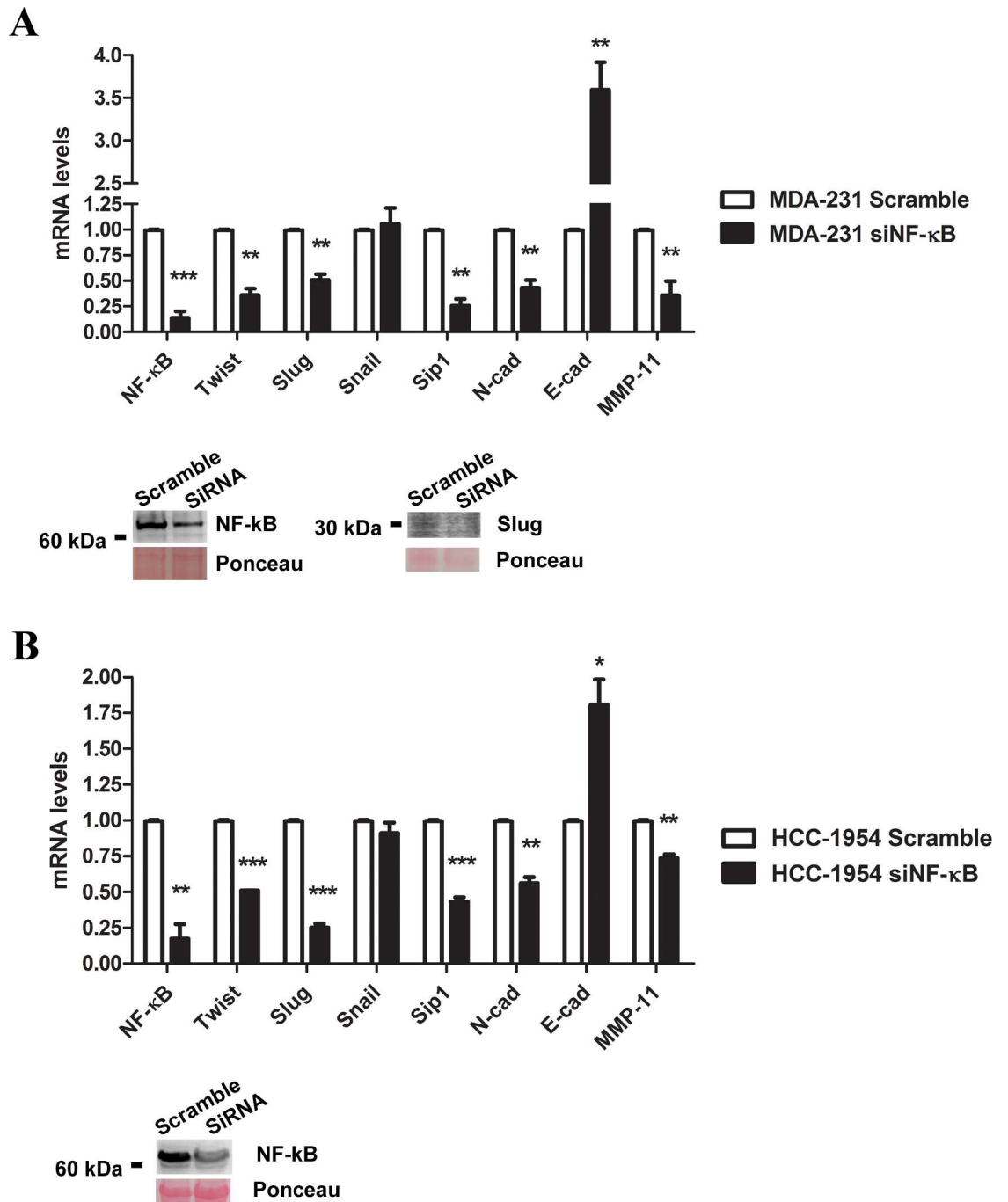
Fig 5. Relative expression of EMT-related genes after NF-κB/p65 genetic silencing using a siRNA approach. The mRNA levels of the EMT-inducing factors *SNAIL1*, *SLUG*, *TWIST1*, and *SIP1* and EMT-phenotype markers *E-CADHERIN*, *N-CADHERIN* and *MMP11* together with NF-κB/p65 inhibition at the protein level were assessed in MDA-MB-231 (A) and HCC-1954 (B) cells (scramble and siNF-κB/p65). Moreover, Slug expression was evaluated at the protein level for MDA-MB-231 by western blot assay in scramble and siNF-κB cells. Ponceau staining was used as a loading control. The data were expressed as the mean ± SD. * = $p<0.05$, ** = $p<0.01$, *** = $p<0.001$.

doi:10.1371/journal.pone.0169622.g005

regulates the TWIST1 promoter at -54 bp, the SLUG promoter at -587 bp and the SIP1 promoter at -769 bp, which could be inhibited by treatment with DHMEQ. Consistent with these
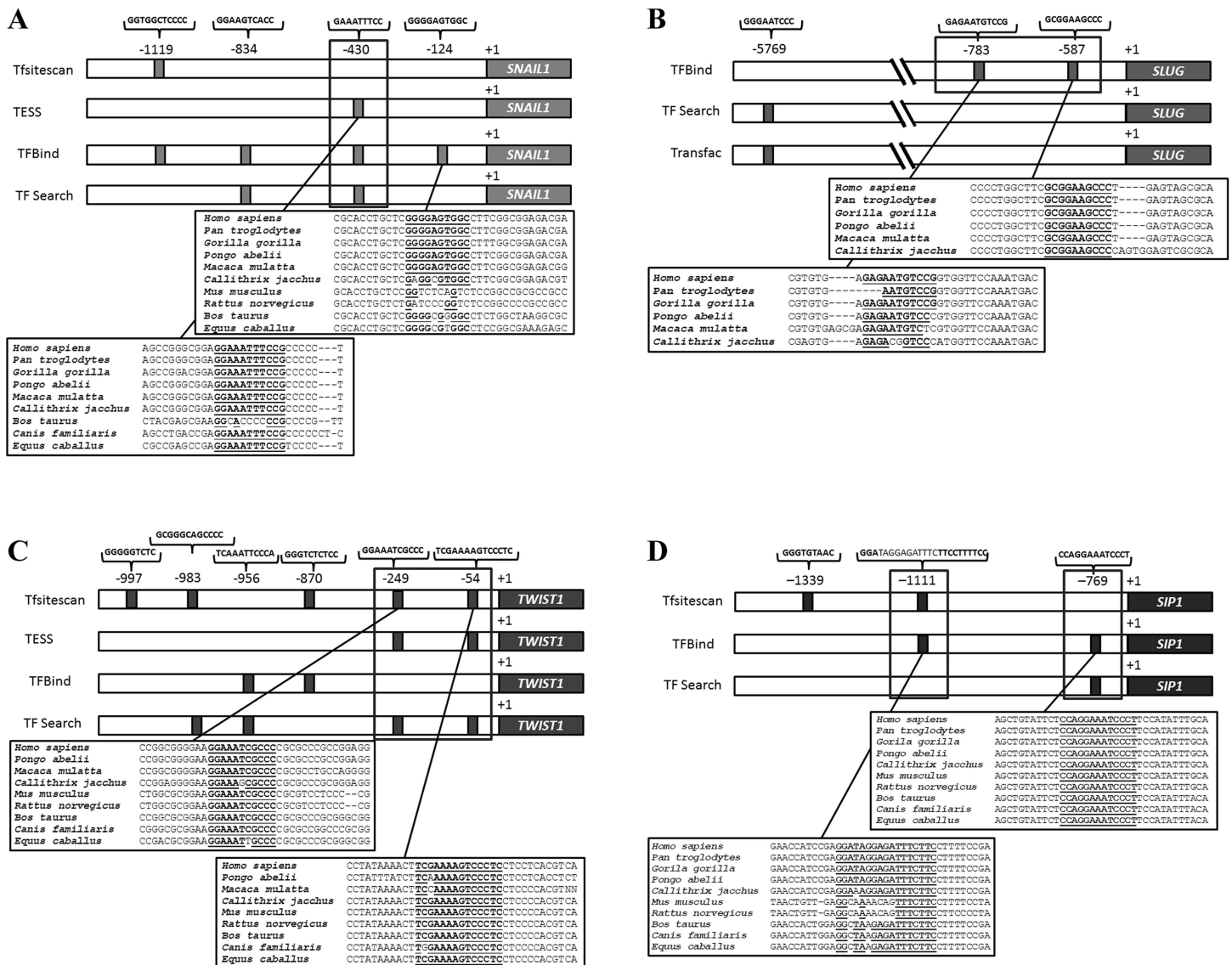
Fig 6. Representative scheme of putative NF-κB binding sites located in the SNAIL1 (A), SLUG (B), TWIST1 (C) and SIP1 (D) promoter regions predicted by Tfsitescan, TESS, TFBind, TFSearch and Transfac bioinformatics tools. An alignment of the DNA region showed evolutionarily conservation among metazoan species. Identical nucleotides are in bold. Gray lines indicate regions investigated by chromatin immunoprecipitation. +1: transcription start site.

doi:10.1371/journal.pone.0169622.g006

observations, NF-κB inhibition (through pharmacological and knockdown approaches) also decreased the mRNA levels of these three TFs (Figs 3 and 5), confirming them as NF-κB/p65 transcriptional targets. Interestingly, our western blot results showed diminished protein levels of NF-κB in DHMEQ treatment (Fig 3). This finding may be explained by the fact that NF-κB autoregulates its expression in a positive feedback loop [57]. As DHMEQ treatment pharmacologically inhibits NF-κB translocation and, consequently, activation, the observed effect could be occurring in breast cancer cells.

In contrast to previous work performed by Barberà et al. [58], our results showed no NF-κB/p65 binding in the Snail1 promoter region. Our differing findings are a result of methodological differences, as Barberà et al. [58] noted a putative NF-κB/p65 responsive region between -194 bp and -78 bp upstream of the transcription start site of this gene without

A
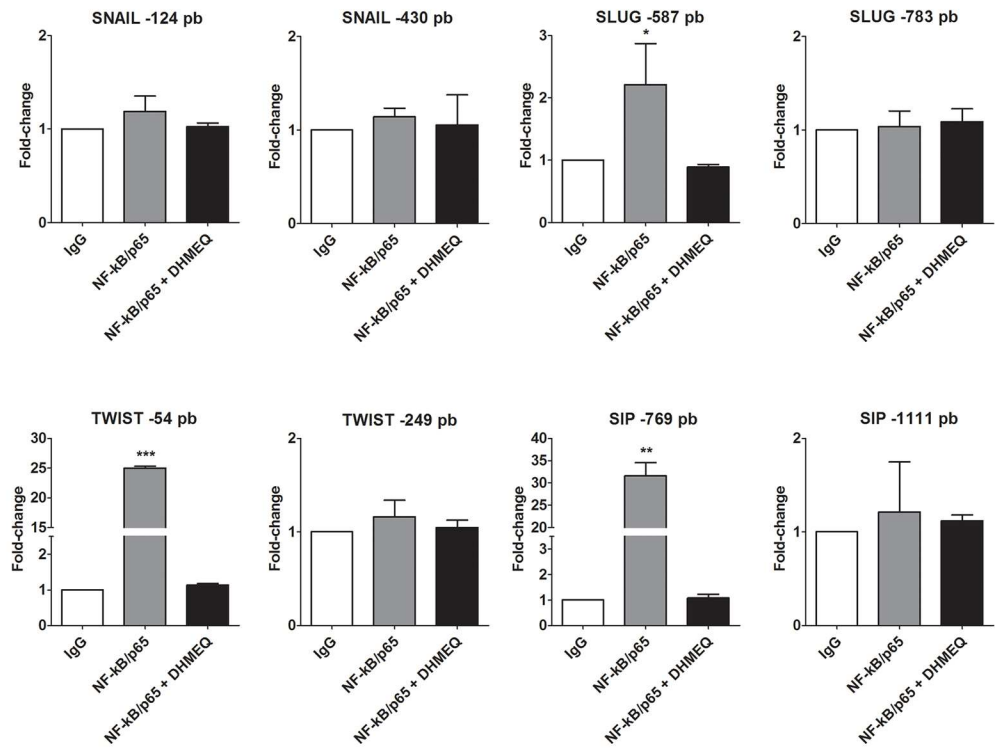
B
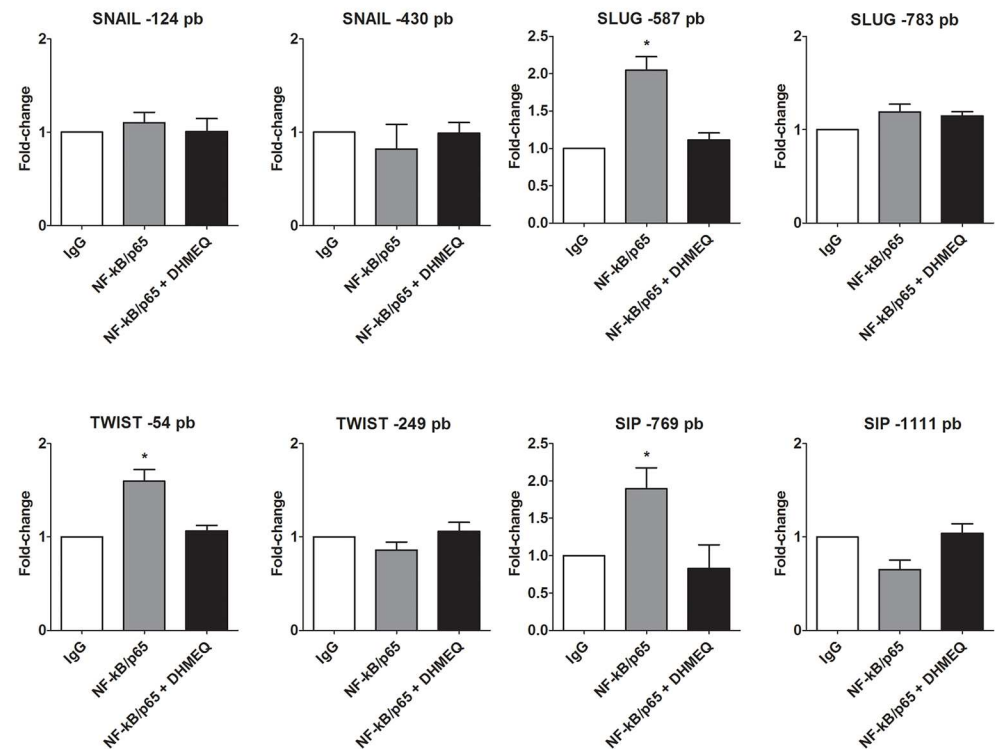
Fig 7. ChIP-qPCR of predicted NF-κB/p65 binding sites in the SNAIL1, SLUG, TWIST1 and SIP1 promoter regions using MDA-MB-231 (A) and HCC-1954 (B) cells. The histograms set a fold-change of each site by comparing the IgG negative control to NF-κB/p65 antibodies with the natural and treated (DHMEQ) condition. The data were expressed as the mean ± SD. * = $p<0.05$, ** = $p<0.01$, *** = $p<0.001$.

doi:10.1371/journal.pone.0169622.g007

describing the specific NF-κB binding site. We conducted a prediction analysis in the same region indicated by Barberà et al. [58] and found a likely binding site for NF-κB in the Snail1 promoter at -124 bp, but it was not confirmed by ChIP-qPCR (Fig 7). Later, the same group was unable to repeat this result in cancer models and claimed that the SNAIL promoter activation by NF-κB seems to be tissue specific [59]. Additionally, the former work and a study published by Katoh and Katoh [60] were not able to identify NF-κB binding sites in the SIP1 promoter, in contrast to our findings (Fig 6D). Regarding SLUG and TWIST1, Storci et al. [61] and Pham et al. [62], respectively, suggested a regulatory role of NF-κB in cancer models, but they did not experimentally demonstrate this mechanism.

Altogether, these results suggest that NF-κB acts directly to promote an aggressive phenotype of breast cancer cells through the transcriptional activation of EMT regulator genes. Our findings may contribute to a greater understanding and identification of the main players involved in the metastatic process in this tumor type. A simple model of the main findings of this work is shown schematically in Fig 9. Therefore, our work helps to reinforce NF-κB as a promising target for cancer therapy, especially for the management of invasive breast cancer.
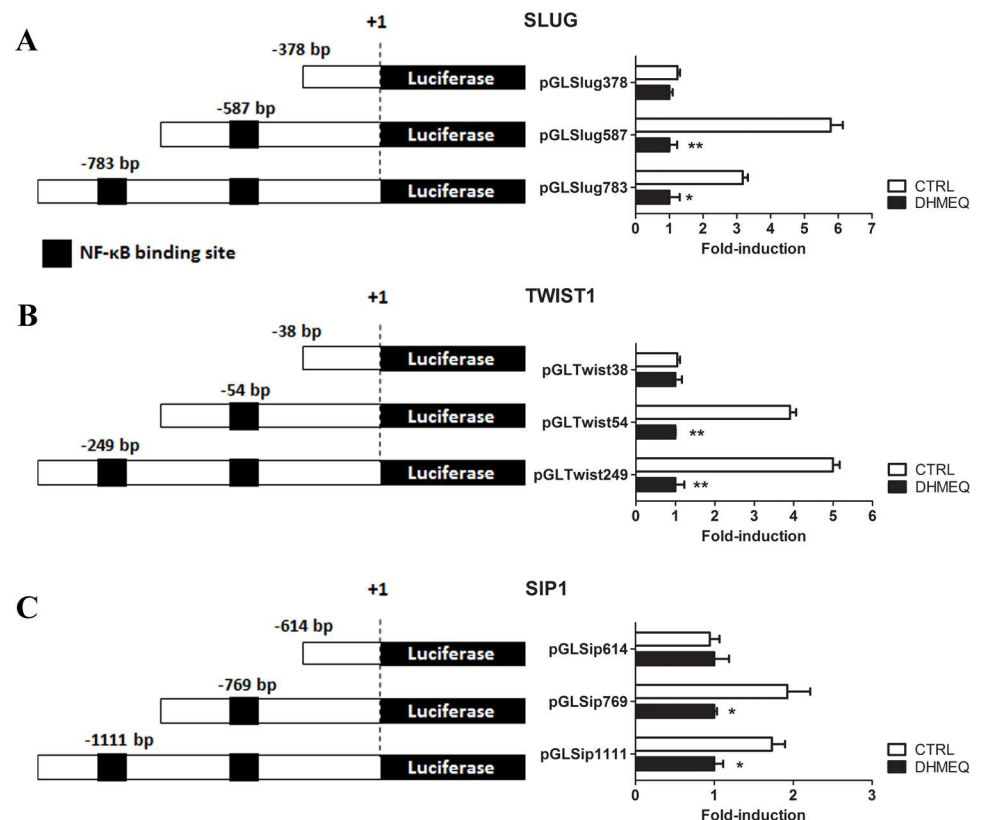
Fig 8. Relative luciferase activity in MDA-MB-231 cells transfected with pGL3-plasmid containing the SLUG (A), TWIST1 (B) and SIP1 (C) promoter regions. The firefly luciferase was normalized to the renilla vector, and the values are relative to the pGL3 (Mock) signal. The black boxes in the schematic representation plasmid constructs represent NF-κB binding sites. The bar graphs represent the relative luciferase activities of each construct in MDA-MB-231 cells, the white bars indicate natural NF-κB expression, and the black bars show NF-κB inhibition through DHMEQ treatment (10 µg/ml for 16 h). Each bar represents the mean ± SD.
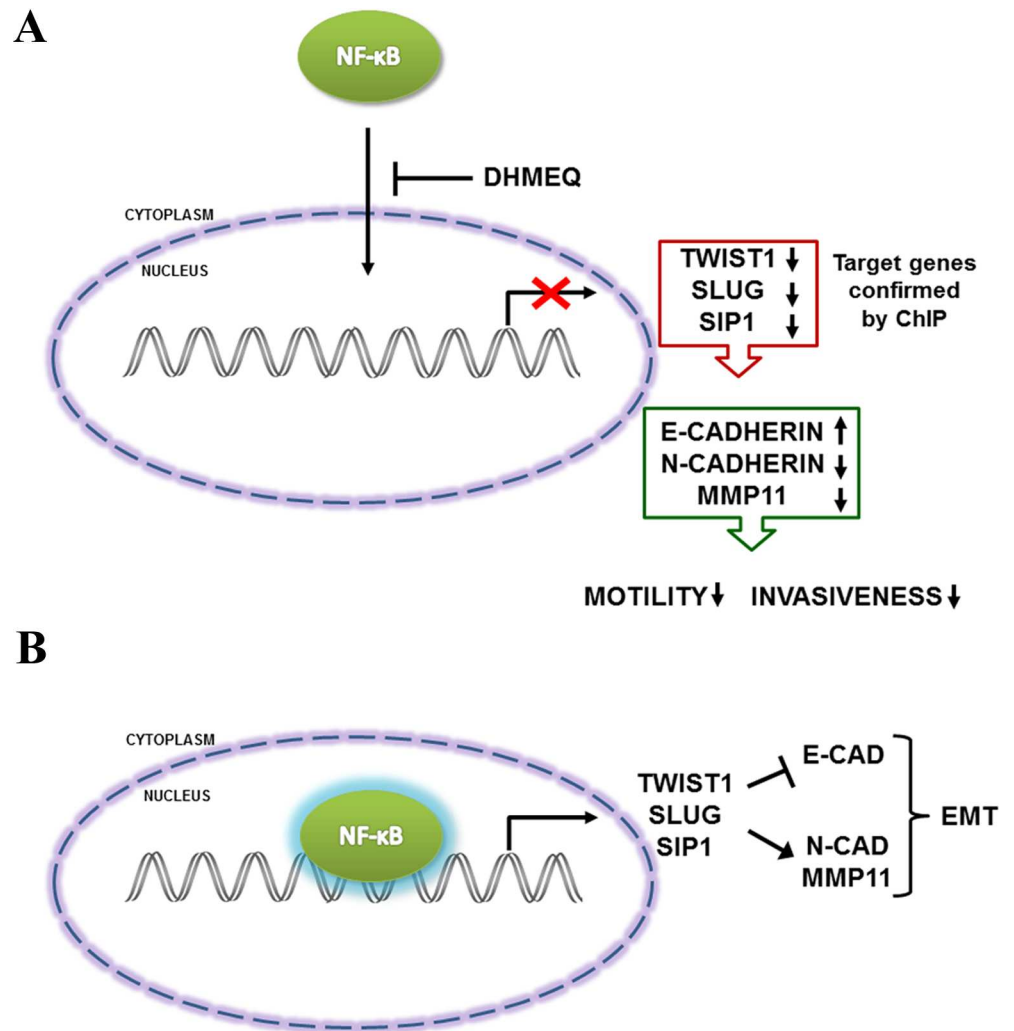
doi:10.1371/journal.pone.0169622.g008

Fig 9. Schematic representation of our findings. A) Inhibition of NF-κB/p65 translocation reduces the expression of EMT-transcription factors that have been shown to regulate target genes of NF-κB. This inhibition increased E-cadherin expression, decreased N-cadherin and MMP11 expression and reduced cell motility and invasiveness potential. B) Then, NF-κB/p65 transcriptionally regulates the promoter regions of TWIST1, SLUG and SIP1, which in turn represses the epithelial marker E-cadherin and activates the mesenchymal markers N-cadherin and MMP11, resulting in induction of the EMT process.

doi:10.1371/journal.pone.0169622.g009

Supporting Information

S1 Table. Primer sequences of the investigated genes.
(DOC)

S2 Table. Primer sequences flanking the predicted NF-κB binding sites.
(DOC)

S1 Fig. NF-κB-luciferase reporter activity comparing the dose-response effects of DHMEQ in MDA-MB-231 (A) HCC-1954 (B) and MCF-7 (C) cells after 16 h of treatment. The firefly luciferase was normalized to the renilla vector, and the values are relative to the pGL3 (Mock) signal. The bar graphs represent the relative luciferase activities of each DHMEQ concentration (3, 10 and 30 μg/ml) in breast cancer cells. Each bar represents the

mean ± SD. * = $p < 0.05$, ** = $p < 0.01$, *** = $p < 0.001$.
(TIF)

S2 Fig. DHMEQ effect on cell viability. The cell viability rate evaluating three treatment conditions (3, 10 and 30 μg/ml of DHMEQ for 24 and 48 h) in MDA-MB-231 (A), HCC-1954 (B) and MCF-7 cells (C) compared to non-treated cells (empty bars). Each bar represents the mean ± SD. * = $p < 0.05$, ** = $p < 0.01$.
(TIF)

S3 Fig. Relative expression of the EMT-related genes and ChIP-qPCR of predicted NF-κB/p65 binding sites using MCF-7 cells. mRNA levels of *SNAIL1*, *SLUG*, *TWIST1*, and *SIP1* (A) together with EMT-phenotype markers, such as *E-CADHERIN*, *N-CADHERIN* and *MMP11* (B), were assessed after 8, 16 and 24 h of DHMEQ treatment. (C) The evaluation of EMT-related genes after genetic silencing of NF-κB/p65. (D) ChIP results of predicted NF-κB/p65 binding sites in *SNAIL1*, *SLUG*, *TWIST1* and *SIP1* promoter regions. The histograms set a fold-change of each site by comparing the IgG negative control to NF-κB/p65 antibodies with the natural and treated (DHMEQ) condition. The data were expressed as the mean ± SD.
(TIF)

Acknowledgments

Author Contributions

Conceptualization: BRBP ALM AMM ESFWA.

Formal analysis: BRBP ALM GMF.

Funding acquisition: ESFWA.

Investigation: BRBP ALM GMF WFS SC.

Methodology: BRBP ALM GMF SC.

Project administration: ESFWA.

Resources: ESFWA JAMD.

Supervision: ESFWA JAMD.

Validation: BRBP ALM GMF WFS SC.

Visualization: BRBP ALM GMF WFS AMM SC ESFWA.

Writing – original draft: BRBP ALM ESFWA.

Writing – review & editing: BRBP ALM GMF SC ESFWA.

References

1. GLOBOCAN. Cancer Incidence and Mortality Worldwide: IARC Cancer Base [Internet]. Lyon, France: International Agency for Research on Cancer. 2012. Available: http://globocan.iarc.fr/Pages/fact_sheets_cancer.aspx. Accessed July 2015

2. World Health Organization. Available: http://www.who.int/mediacentre/factsheets/fs297/en/ Accessed July 2015

3. Huber MA, Kraut N, Beug H. Molecular requirements for epithelial-mesenchymal transition during tumor progression. Curr Opin Cell Biol. 2005; 17(5):548–58. doi: 10.1016/j.ceb.2005.08.001 PMID: 16098727

4. Cano A, Pérez-Moreno MA, Rodrigo I, Locascio A, Blanco MJ, del Barrio MG, et al. The transcription factor snail controls epithelial–mesenchymal transitions by repressing E-cadherin expression. Nat Cell Biol. 2000; 2(2):76–83. doi: 10.1038/35000025 PMID: 10655586

5. Batlle E, Sancho E, Francí C, Domínguez D, Monfar M, Baulida J, de Herreros AG. The transcription factor snail is a repressor of E-cadherin gene expression in epithelial tumour cells. Nat Cell Biol. 2000; 2(2):84–89. doi: 10.1038/35000034 PMID: 10655587

6. Bolós V, Peinado H, Pérez-Moreno MA, Fraga MF, Esteller M, Cano A. The transcription factor Slug represses E-cadherin expression and induces epithelial to mesenchymal transitions: a comparison with Snail and E47 repressors. J Cell Sci. 2003; 116(3):499–511.

7. Yang J, Mani SA, Donaher JL, Ramaswamy S, Itzykson RA, Come C. Twist, a master regulator of morphogenesis, plays an essential role in tumor metastasis. Cell. 2004; 117(7):927–39. doi: 10.1016/j.cell.2004.06.006 PMID: 15210113

8. Comijn J, Berx G, Vermassen P, Verschueren K, van Grunsven L, Bruyneel E, et al. The two-handed E box binding zinc finger protein SIP1 downregulates E-cadherin and induces invasion. Mol Cell. 2001; 7 (6):1267–78. PMID: 11430829

9. Vandewalle C, Comijn J, De Craene B, Vermassen P, Bruyneel E, Andersen H, et al. SIP1/ZEB2 induces EMT by repressing genes of different epithelial cell–cell junctions. Nucleic Acids Res. 2005; 33 (20):6566–78. doi: 10.1093/nar/gki965 PMID: 16314317

10. Blanco MJ, Moreno-Bueno G, Sarrio D, Locascio A, Cano A, Palacios J, Nieto MA. Correlation of Snail expression with histological grade and lymph node status in breast carcinomas. Oncogene. 2002; 21 (20):3241–46. doi: 10.1038/sj.onc.1205416 PMID: 12082640

11. Martin TA, Goyal A, Watkins G, Jiang WG. Expression of the transcription factors snail, slug, and twist and their clinical significance in human breast cancer. Ann Surg Oncol. 2005; 12(6):488–96. doi: 10.1245/ASO.2005.04.010 PMID: 15864483

12. Xu Y, Hu B, Qin L, Zhao L, Wang Q, Wang Q, Jiang J. SRC-1 and Twist1 expression positively correlates with a poor prognosis in human breast cancer. Int J Biol Sci. 2014; 10(4):396–403. doi: 10.7150/ijbs.8193 PMID: 24719557

13. Ip YT, Park RE, Kosman D, Yazdanbakhsh K, Levine M. Dorsal-twist interactions establish *snail* expression in the presumptive mesoderm of the *Drosophila* embryo. Genes Dev. 1992; 6(8):1518–30. PMID: 1644293

14. Furlong EE, Andersen EC, Null B, White KP, Scott MP. Patterns of gene expression during *Drosophila* mesoderm development. Science. 2001; 293(5535):1629–33. doi: 10.1126/science.1062660 PMID: 11486054

15. Gilmore TD, Garbati MR. Inhibition of NF-κB signaling as a strategy in disease therapy. Curr Top Microbiol Immunol. 2010; 349:245–263.

16. Zheng C, Yin Q, Wu H. Structural studies of NF-κB signaling. Cell Res. 2011; 21(1):183–95. doi: 10.1038/cr.2010.171 PMID: 21135870

17. Umezawa K. Inhibition of tumor growth by NF-kappaB inhibitors. Cancer Sci. 2006; 97(10): 990–5. doi: 10.1111/j.1349-7006.2006.00285.x PMID: 16925581

18. Gupta SC, Sundaram C, Reuter S, Aggarwal BB. Inhibiting NF-κB activation by small molecules as a therapeutic strategy. Biochim Biophys Acta. 2010; 1799:775–87. doi: 10.1016/j.bbagrm.2010.05.004 PMID: 20493977

19. Pires BR, Mencalha AL, Abdelhay E. Molecular Mechanisms of NF-kB on Cancer Promotion and Progression. Journal of the Senologic International Society. 2013; 2(1).

20. Neil RJ, Schiemann WP.Altered TAB1:IKK Interaction Promotes TGF-β-Mediated NF-κB Activation During Breast Cancer Progression. Cancer Res. 2008; 68(5): 1462–70. doi: 10.1158/0008-5472.CAN-07-3094 PMID: 18316610

21. Zhang Q, Helfand BT, Jang TL, Zhu LJ, Chen L, Yang XJ, et al. Nuclear factor-kappaB-mediated transforming growth factor-beta-induced expression of vimentin is an independent predictor of biochemical recurrence after radical prostatectomy. Clin Cancer Res. 2009; 15(10):3557–67. doi: 10.1158/1078-0432.CCR-08-1656 PMID: 19447876

22. Pantuck AJ, An J, Liu H, Rettig MB. NF-kappaB-dependent plasticity of the epithelial to mesenchymal transition induced by Von Hippel-Lindau inactivation in renal cell carcinomas. Cancer Res. 2010; 70(2): 752–61. doi: 10.1158/0008-5472.CAN-09-2211 PMID: 20068166

23. Chung CH, Parker JS, Ely K, Carter J, Yi Y, Murphy BA, et al. Gene expression profiles identify epithelial-to-mesenchymal transition and activation of nuclear factor-kappaB signaling as characteristics of a

high-risk head and neck squamous cell carcinoma. Cancer Res. 2006; 66(16):8210–18. doi: 10.1158/0008-5472.CAN-06-1213 PMID: 16912200

24. Matsumoto N, Ariga A, To-e S, Nakamura H, Agata N, Hirano S, et al. Synthesis of NF-kappaB activation inhibitors derived from epoxyquinomicin C. Bioorg Med Chem Lett. 2000; 10(9):865–9. PMID: 10853648

25. Umezawa K, Chaicharoenpong C. Molecular design and biological activities of NF-kappaB inhibitors. Mol Cells. 2002; 14(2):163–7. PMID: 12442886

26. Watanabe M, Nakashima M, Togano T, Higashihara M, Watanabe T, Umezawa K, Horie R. Identification of the RelA domain responsible for action of a new NF-kappaB inhibitor DHMEQ. Biochem Biophys Res Commun. 2008; 376(2):310–4. doi: 10.1016/j.bbrc.2008.08.148 PMID: 18782563

27. Matsumoto G, Namekawa J, Muta M, Nakamura T, Bando H, Tohyama K, et al. Targeting of nuclear factor kappaB Pathways by dehydroxymethylepoxyquinomicin, a novel inhibitor of breast carcinomas: antitumor and antiangiogenic potential in vivo. Clin Cancer Res. 2005; 11(3):1287–93. PMID: 15709200

28. Kikuchi E, Horiguchi Y, Nakashima J, Kuroda K, Oya M, Ohigashi T, et al. Suppression of hormone-refractory prostate cancer by a novel nuclear factor kappaB inhibitor in nude mice. Cancer Res. 2003; 63(1):107–10. PMID: 12517785

29. Horiguchi Y, Kuroda K, Nakashima J, Murai M, Umezawa K. Antitumor effect of a novel nuclear factor-kappa B activation inhibitor in bladder cancer cells. Expert Rev Anticancer Ther. 2003; 3(6):793–8 doi: 10.1586/14737140.3.6.793 PMID: 14686701

30. Starenki DV, Namba H, Saenko VA, Ohtsuru A, Maeda S, Umezawa K, Yamashita S. Induction of thyroid cancer cell apoptosis by a novel nuclear factor kappaB inhibitor, dehydroxymethylepoxyquinomicin. Clin Cancer Res. 2004; 10(20):6821–9. doi: 10.1158/1078-0432.CCR-04-0463 PMID: 15501958

31. Matsumoto G, Muta M, Umezawa K, Suzuki T, Misumi K, Tsuruta K, Okamoto A, Toi M. Enhancement of the caspase-independent apoptotic sensitivity of pancreatic cancer cells by DHMEQ, an NF-kappaB inhibitor. Int J Oncol. 2005; 27(5):1247–55. PMID: 16211219

32. Ruan HY, Masuda M, Ito A, Umezawa K, Nakashima T, Yasumatsu R, et al. Effects of a novel NF-kappaB inhibitor, ehydroxymethylepoxyquinomicin (DHMEQ), on growth, apoptosis, gene expression, and chemosensitivity in head and neck squamous cell carcinoma cell lines. Head Neck. 2006; 28(2):158–65. doi: 10.1002/hed.20304 PMID: 16355386

33. Watanabe M, Dewan MZ, Okamura T, Sasaki M, Itoh K, Higashihara M, et al. A novel NF-kappaB inhibitor DHMEQ selectively targets constitutive NF-kappaB activity and induces apoptosis of multiple myeloma cells in vitro and in vivo. Int J Cancer. 2005; 114(1):32–8. doi: 10.1002/ijc.20688 PMID: 15523684

34. Ohsugi T, Kumasaka T, Okada S, Ishida T, Yamaguchi K, Horie R, et al. Dehydroxymethylepoxyquinomicin (DHMEQ) therapy reduces tumor formation in mice inoculated with tax-deficient adult T-cell leukemia-derived cell lines. Cancer Lett. 2007; 257(2):206–15. doi: 10.1016/j.canlet.2007.07.017 PMID: 17764832

35. Rodriguez LG, Wu Xiaoyang, Guan Jun-Lin. Wound-Healing Assay. In: Guan J-L (ed) Methods in Molecular Biology, vol. 294: Cell Migration: Developmental Methods and Protocols. Humana Press Inc., Totowa, NJ; 2002.

36. Livak KJ, Schmittgen TD. Analysis of relative gene expression data using real-time quantitative PCR and the 2-ΔΔCT method. Methods. 2001; 25:402–8. doi: 10.1006/meth.2001.1262 PMID: 11846609

37. Mencalha AL, Binato R, Ferreira GM, Du Rocher B, Abdelhay E. Forkhead box M1 (FoxM1) gene is a new STAT3 transcriptional factor target and is essential for proliferation, survival and DNA repair of K562 cell line. PLoS One; 2012; 7(10):e48160. doi: 10.1371/journal.pone.0048160 PMID: 23110199

38. Taneyhill LA, Adams MS. Investigating regulatory factors and their DNA binding affinities through real time quantitative PCR (RT-QPCR) and chromatin immunoprecipitation (ChIP) assays. Methods Cell Biol. 2008; 87:367–89. doi: 10.1016/S0091-679X(08)00219-7 PMID: 18485307

39. Zhou R, Li X, Hu G, Gong AY, Drescher KM, Chen XM. miR-16 targets transcriptional corepressor SMRT and modulates NF-kappaB-regulated transactivation of interleukin-8 gene. PLoS One. 2012; 7 (1), e30772 doi: 10.1371/journal.pone.0030772 PMID: 22292036

40. Geiger TR, Peeper DS. Metastasis mechanisms. Biochim Biophys Acta. 2009; 1796(2):293–308. doi: 10.1016/j.bbcan.2009.07.006 PMID: 19683560

41. De Craene B, Berx G. Regulatory networks defining EMT during cancer initiation and progression. Nat Rev Cancer. 2013; 13(2):97–110. doi: 10.1038/nrc3447 PMID: 23344542

42. Brabletz T. To differentiate or not-routes towards metastasis. Nat Rev Cancer. 2012; 12(6):425–36. doi: 10.1038/nrc3265 PMID: 22576165

43. Huber MA, Azoitei N, Baumann B, Grünert S, Sommer A, Pehamberger H, et al. NF-kappaB is essential for epithelial-mesenchymal transition and metastasis in a model of breast cancer progression. J Clin Invest. 2004; 114(4):569–81. doi: 10.1172/JCI21358 PMID: 15314694

44. Park BK, Zhang H, Zeng Q, Dai J, Keller ET, Giordano T, et al. NF-kappaB in breast cancer cells promotes osteolytic bone metastasis by inducing osteoclastogenesis via GM-CSF. Nat Med. 2007; 13 (1):62–9. doi: 10.1038/nm1519 PMID: 17159986

45. Narasimhan M, Ammanamanchi S. Curcumin blocks RON tyrosine kinase-mediated invasion of breast carcinoma cells. Cancer Res. 2008; 68(13):5185–92 doi: 10.1158/0008-5472.CAN-07-6883 PMID: 18593918

46. Hinohara K, Kobayashi S, Kanauchi H, Shimizu S, Nishioka K, Tsuji E, et al. ErbB receptor tyrosine kinase/NF-kB signaling controls mammosphere formation in human breast cancer. Proc Natl Acad Sci USA. 2012; 109(17):6584–9. doi: 10.1073/pnas.1113271109 PMID: 22492965

47. Maier HJ, Schmidt-Strassburger U, Huber MA, Wiedemann EM, Beug H, Wirth T. NF-kappaB promotes epithelial-mesenchymal transition, migration and invasion of pancreatic carcinoma cells. Cancer Lett. 2010; 295(2):214–28. doi: 10.1016/j.canlet.2010.03.003 PMID: 20350779

48. Pantuck AJ, An J, Liu H, Rettig MB. NF-kappaB-dependent plasticity of the epithelial to mesenchymal transition induced by Von Hippel-Lindau inactivation in renal cell carcinomas. Cancer Res. 2010; 70 (2):752–61. doi: 10.1158/0008-5472.CAN-09-2211 PMID: 20068166

49. Chung CH, Parker JS, Ely K, Carter J, Yi Y, Murphy BA, et al. Gene expression profiles identify epithelial-to-mesenchymal transition and activation of nuclear factor-kappaB signaling as characteristics of a high-risk head and neck squamous cell carcinoma. Cancer Res. 2006; 66(16):8210–18. doi: 10.1158/0008-5472.CAN-06-1213 PMID: 16912200

50. Zhang C, Klymkowsky MW. Unexpected functional redundancy between *Twist* and *Slug* (*Snail2*) and their feedback regulation of NF-kappaB via Nodal and Cerberus. Dev Biol. 2009; 331(2):340–9. doi: 10.1016/j.ydbio.2009.04.016 PMID: 19389392

51. Liu X, Huang S, Ma J, Li C, Zhang Y, Luo, L. NF-κB and Snail1a coordinate the cell cycle with gastrulation. J Cell Biol. 2009; 184(6):805–15. doi: 10.1083/jcb.200806074 PMID: 19307597

52. Blick T, Widodo E, Hugo H, Waltham M, Lenburg ME, Neve RM, et al. Epithelial mesenchymal transition traits in human breast cancer cell lines. Clin Exp Metastasis. 2008; 25(6):629–42. doi: 10.1007/s10585-008-9170-6 PMID: 18461285

53. Holliday DL, Speirs V. Choosing the right cell line for breast cancer research. Breast Cancer Res. 2011; 13(4):215. doi: 10.1186/bcr2889 PMID: 21884641

54. Vesuna F, Lisok A, Kimble B, Domek J, Kato Y, van der Groep P, et al. *Twist* contributes to hormone resistance in breast cancer by downregulating estrogen receptor-α. Oncogene.2012; 31(27):3223–34. doi: 10.1038/onc.2011.483 PMID: 22056872

55. Huber MA, Beug H, Wirth T. Epithelial-mesenchymal transition: NF-kappaB takes center stage. Cell Cycle. 2004; 3(12):1477–80. doi: 10.4161/cc.3.12.1280 PMID: 15539952

56. Kang Y, Massagué J. Epithelial-mesenchymal transitions: twist in development and metastasis. Cell. 2004; 118(3):277–9. doi: 10.1016/j.cell.2004.07.011 PMID: 15294153

57. Sun SC, Ganchi PA, Beraud C, Ballard DW, Greene WC. Autoregulation of the NF-kappa B transactivator RelA (p65) by multiple cytoplasmic inhibitors containing ankyrin motifs. Proc Natl Acad Sci USA. 1994; 91(4):1346–50. PMID: 8108414

58. Barberà MJ, Puig I, Domínguez D, Julien-Grille S, Guaita-Esteruelas S, Peiró S, et al. Regulation of Snail transcription during epithelial to mesenchymal transition of tumor cells; Oncogene. 2004; 23 (44):7345–54. doi: 10.1038/sj.onc.1207990 PMID: 15286702

59. Julien S, Puig I, Caretti E, Bonaventure J, Nelles L, van Roy F, Dargemont C, et al. Activation of NF-kappaB by *Akt* upregulates *Snail* expression and induces epithelium mesenchyme transition. Oncogene. 2007; 26(53):7445–56. doi: 10.1038/sj.onc.1210546 PMID: 17563753

60. Katoh M, Katoh M. Integrative genomic analyses of *ZEB2*: Transcriptional regulation of *ZEB2* based on SMADs, ETS1, HIF1alpha, POU/OCT, and NF-kappaB. Int J Oncol. 2009; 34(6):1737–42. PMID: 19424592

61. Storci G, Sansone P, Mari S, D'Uva G, Tavolari S, Guarnieri T, et al. TNFalpha up-regulates SLUG via the NF-kappaB/HIF1alpha axis, which imparts breast cancer cells with a stem cell-like phenotype. J Cell Physiol. 2010; 225(3):682–91. doi: 10.1002/jcp.22264 PMID: 20509143

62. Pham CG, Bubici C, Zazzeroni F, Knabb JR, Papa S, Kuntzen C, Franzoso G. Upregulation of Twist-1 by NF-kappaB blocks cytotoxicity induced by chemotherapeutic drugs. Mol Cell Biol. 2007; 27 (11):3920–35 doi: 10.1128/MCB.01219-06 PMID: 17403902